Photonic Crystals

DOI: 10.1002/anie.201104480

Robust Chirped Photonic Crystals Created by Controlled Colloidal Diffusion**

Shin-Hyun Kim, Woong Chan Jeong, Hyerim Hwang, and Seung-Man Yang**

The spontaneous crystallization of monodisperse or bidisperse colloidal particles subject to interparticle interactions enables formation of various three-dimensional (3D) photonic crystal structures,[1] which are promising for biosensors,[2] tunable organic lasers,[3] and color pigments for displays.[4] Therefore, colloidal photonic crystals have long been studied, focusing on wide-area production with a low defect density,[5] controlled embedding of active defects,[6] and patterning of colloidal crystals with discrete colors[7] to accomplish their practical uses.[8] As a new class of 3D photonic materials with advanced functionalities, colloidal crystals having continuous changes in the lattice constants have been reported,[9] which can provide useful properties based on continuously varying stop band wavelengths along the gradient. However, lack of practical technologies to produce such materials with high crystal stability and high controllability over the gradient severely limits their applications.

Here, we report a novel and pragmatic strategy for creating continuous changes in the lattice constant of a 3D photonic crystal using colloidal diffusion in a photocurable medium. The repulsive interparticle potentials accelerated the colloid diffusion by the order of 10^5, $O(10^5)$, relative to dilute hard-sphere colloids, and fast consolidation of the suspension medium captured and solidified the variations in the stop band position as a function of the diffusion distance to produce a chirped 3D photonic crystal (CPhC). By combining the CPhC functionality with a conventional CMOS sensor array, we demonstrated a miniaturized on-chip spectrometer system with a minimum resolution of 0.09 nm in the visible spectral range.

The diffusivity D_0 of colloids in a dilute suspension is described using the Stokes–Einstein law, $D_0 = kT/3\pi\eta d$, where the displacement length is proportional to the square root of time, $O(D_0 t)^{1/2}$, k is the Boltzmann constant, T is temperature, η is the viscosity of the continuous phase, and d is the diameter of the particles. In a concentrated suspension, by contrast, the diffusivity can vary significantly from D_0 because of interparticle interactions. When a concentrated suspension of colloidal particles that interact through a highly repulsive potential is placed in contact with a dilute suspension, the high osmotic pressure dramatically accelerates the diffusion of colloids, which overcomes the opposing flow of the continuous phase.[10] Simultaneously, the repulsive colloids form a crystal lattice to reduce the total interparticle interaction energy. Because the volume fraction of colloids determines the lattice constant of the crystals, gradient diffusion facilitates generation of a gradual increase in the lattice constants along the diffusion direction, resulting in a CPhC material.

CPhC films were prepared for practical use by using a photocurable silica suspension of ethoxylated trimethylolpropane triacrylate (ETPTA) with a high polarity and refractive index ($n_{\mathrm{ETPTA}} = 1.4689$) comparable to that of the colloidal silica particles ($n_{\mathrm{silica}} = 1.45$); small index contrast induces small van der Waals attraction between particles. Under a repulsive interparticle potential which is contributed from the disjoining pressure of the solvation layer[11] and weak electrostatic interactions, silica particles formed non-close-packed crystals in a state of concentrated suspension. When the concentrated silica–ETPTA suspension was introduced by capillary action into microchannels that were prefilled with a particle-free ETPTA solution, the silica particles along the front of the concentrated suspension experienced relatively strong forces because of the unbalanced repulsive forces from neighboring particles. The force imbalance resulted in a migration of particles to form a concentration gradient. This diffusion process completely ceased once the suspension medium was solidified by photopolymerization, thereby producing a composite CPhC film with a color gradient. The porous CPhC film could also be prepared by the selective removal of silica particles. This method provided a higher reflectivity and a larger bandwidth at the stop band. The processes by which the CPhC films were prepared are schematically summarized in Figure 1 a–d. A schematic illustration and a photograph of a miniaturized spectrometer device are shown in Figure 1 e as promising applications of the CPhC materials.

Figure 2 a shows an optical microscopy image of a porous CPhC film with a reflection color gradient, prepared by the diffusion of silica particles over 7 h, and Figure 2 b shows scanning electron microscopy (SEM) images of crystal cross-sections at the positions indicated by the dashed lines; a silica–ETPTA suspension of particle diameter d of 177 nm and volume fraction ϕ of 0.33 was used. Because crystalliza-

[*] Dr. S.-H. Kim, W. C. Jeong, H. Hwang, Prof. S.-M. Yang
National Creative Research Initiative Center for
Integrated Optofluidic Systems and Department of Chemical and Biomolecular Engineering, KAIST, Daejeon, 305-701 (Korea)
E-mail: dmz@kaist.ac.kr
smyang@kaist.ac.kr
Homepage: http://msfl.kaist.ac.kr

[**] This work was supported by a grant from the Creative Research Initiative Program of the Ministry of Education, Science, and Technology for "Complementary Hybridization of Optical and Fluidic Devices for Integrated Optofluidic Systems." We thank Dr. Se-Heon Kim at the California Institute of Technology for useful discussions.

Supporting information for this article is available on the WWW under http://dx.doi.org/10.1002/anie.201104480.

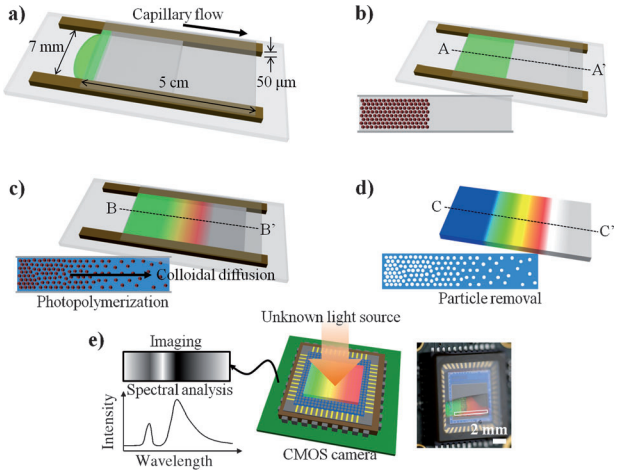

Figure 1. a–d) Schematic illustration of the preparation of a chirped 3D photonic crystal (CPhC). a,b) A concentrated silica–ETPTA suspension was introduced into the microchannel prefilled with a particle-free ETPTA solution. c) Gradient diffusion of the repulsive silica particles created a concentration gradient along the direction of diffusion, and fast solidification of the photocurable medium enabled the preparation of a composite CPhC film. d) Selective etching of the silica particles yielded a porous CPhC film. e) A composite CPhC film mounted on a CMOS sensor array can be used to create a miniaturized spectrometer. A photograph of the device is included. The white box indicates the imaging area for spectral analysis.

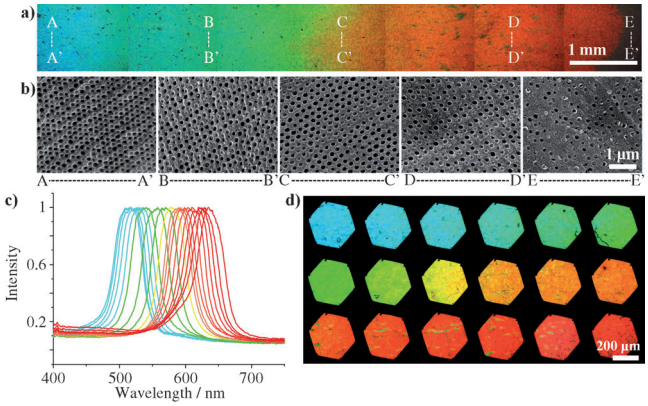

Figure 2. a,b) Optical microscopy image of the porous CPhC film and SEM images of cross-sections at the positions indicated by the dashed lines. The film was prepared by diffusion of 177 nm silica particles over 7 h. c,d) Reflectance spectra and the corresponding optical microscopy images of the porous film at distance intervals of 0.45 mm along the diffusion direction.

tion began at the confining walls, the densest plane of the face-centered-cubic (fcc) lattice, the (111) plane, formed along the surfaces of the microchannel. Therefore, the resulting reflection colors corresponded to the L-gap. The SEM images show a decrease in the volume fraction of the air cavities and a concomitant increase in the lattice constant along the diffusion direction. Therefore, the film showed a gradual change in the reflection color from blue to red. The rightmost region did not show a reflection color because of the absence of void ordering, as shown in the last SEM image.

The reflectance spectra and their corresponding optical microscopy images are shown in Figure 2c,d, respectively. The images and spectra were collected at local areas of hexagonal dots with 190 μm in dimension at distance intervals of 0.45 mm along the gradient direction. The reflection intensity exceeded 80% over the whole area, and the average full-width-at-half-maximum (FWHM) was 46 nm. The bandgap effects of the CPhC film were investigated by incorporating fluorescent dye molecules into the colloidal suspension before ETPTA infiltration, then forming a dye-doped porous CPhC film. The photoluminescence spectrum of the dye depended on the position along the porous CPhC film is shown in Figure S1 of the Supporting Information. Emission was inhibited at the bandgap because of a low photon density of states (DOS), and emission was enhanced at the band edge because of a high DOS. This variability caused a dip in the emission spectrum, and the dip position shifted to longer wavelengths as the excitation volume was shifted along the gradient direction, when the bandgap overlapped with the spontaneous emission spectrum of the dye molecules.[12]

A sample undergoing gradient diffusion exists in a non-steady state until it arrives at a constant concentration profile throughout the volume. Therefore, the diffusion time is critical for determining the slope of stop band evolution as a function of distance along the gradient, as shown in Figure 3a; the suspensions infiltrated in the microchannel were polymerized after the indicated times prior to dissolution of the silica. The films formed after diffusion times of 5 and 10 min showed a clear boundary between the concentrated and dilute regions, and the boundary became indistinct after 15 min (a slope of 85.6 $nm\,mm^{-1}$). After 20 min, the film showed a color gradient over a distance of 2 mm, with a relatively low density of decolored regions (a slope of 52.5 $nm\,mm^{-1}$). The decolorized area density increased for longer diffusion times, as shown in the image of a sample prepared with a diffusion time of 40 min (a slope of 30.3 $nm\,mm^{-1}$), then decreased slowly over diffusion times up to 7 h to yield a color gradient with a high reflection intensity exceeding 80% throughout the whole gradient area (a slpoe of 13.8 $nm\,mm^{-1}$). Figure 3b summarizes the evolution of the stop band position as a function of the diffusion distance for various diffusion times. The reflectivity increased over the course of diffusion, as shown in Figure 3c, which can be attributed to the enhanced degree of ordering throughout the local rearrangement of the colloids.

Gradient diffusion is a complex process because the diffusivity of each particle depends on the configuration of the neighboring particles. Each particle experiences a different diffusivity at any instant in time. Therefore, particle diffusivity is difficult to model theoretically. Instead, the average diffusivity can be estimated from experimental results. Because the stop band position depends on the particle concentration, as shown in Bragg's law in the Supporting Information, the evolution of the stop band as a function of position, as shown in Figure 3b, is used to calculate the concentration profile, as shown in Figure 3d. Fitting the concentration profiles at each time with the 1D diffusion equation with a constant planar source provided a rough

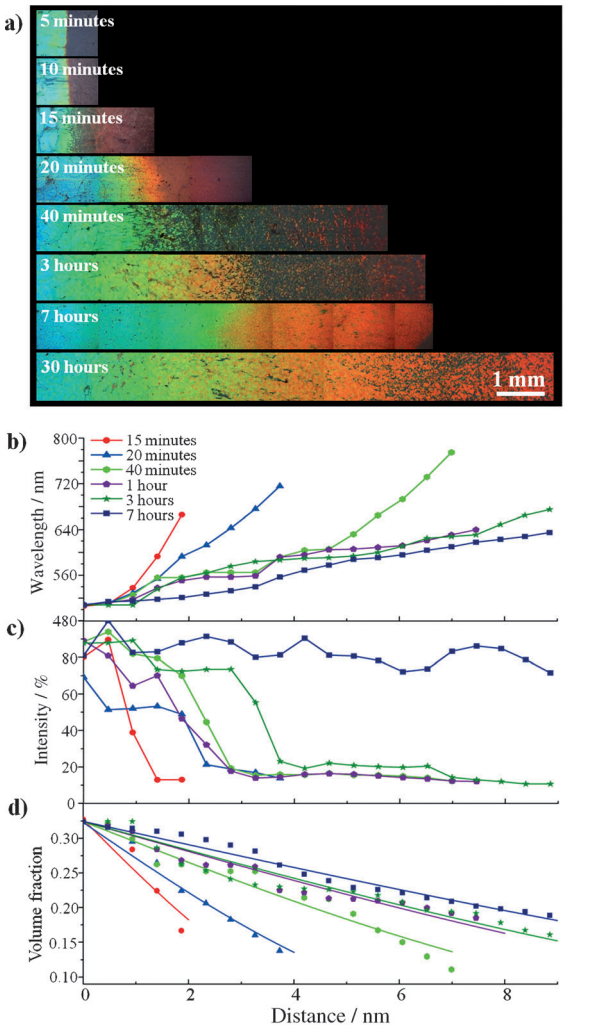

Figure 3. a) Optical microscopy images showing the color gradient of the porous CPhC films prepared by diffusion of 177 nm silica particles for various diffusion times: 5 min, 10 min, 15 min, 20 min, 40 min, 3 h, 7 h, and 30 h. (b–d) The evolution of b) the reflectance peak wavelength, c) reflectivity, and d) void volume fraction, as a function of the distance from the starting position of the gradient for various diffusion times.

estimate of the average diffusivity. The solution is expressed as an error function,

$$\phi(x, t > 0) = \phi_0 \mathrm{erfc}\left(\frac{x}{\sqrt{4Dt}}\right)$$

where ϕ_0 and x are the volume fraction at a constant planar source and distance from the source, respectively. The experimental profiles did not precisely match the equation, as shown in the curves in Figure 3d, because of the variations in the diffusivity of each particle over time. However, the values extracted from the fit functions provided an estimate of the average diffusivities of $O(10^{-9}$–$10^{-8}\,m^2s^{-1})$, which were larger than the Stokes–Einstein coefficient ($10^{-14}\,m^2s^{-1}$) by a factor of 10^5–10^6. The significant increase in the diffusivity was attributed to the high osmotic pressure induced by interparticle repulsion. The average diffusivities were estimated to be 4.43×10^{-9}, 1.02×10^{-8}, 1.57×10^{-8}, 1.97×10^{-8}, 7.13×10^{-9}, and $4.70\times10^{-9}\,m^2s^{-1}$ for 15 min, 20 min, 40 min, 1 h, 3 h, and 7 h, respectively. At the beginning of the gradient diffusion process, only particles on the front of the concentrated suspension experienced an unequal force that resulted in diffusion because of the locally unbalanced repulsive forces. Therefore, the overall movement of the particles was not rapid. The average diffusivity increased up to 1 h, during which time the unbalanced repulsive forces spread throughout the gradient. A reduction in the repulsive forces because of an increase in the interparticle distance slowed the diffusion after 1 h.

Spatially modulated transmission spectra are useful as novel optical filters to create miniaturized spectroscopic instruments.[13] Using the composite CPhC films mounted on a complementary metal-oxide-semiconductor (CMOS) sensor array, we demonstrated a miniaturized spectrometer, as shown in Figure 1e. Unlike conventional spectroscopy, which uses gratings and a long light path, the proposed device uses a CPhC film as an optical filter, over which the transmission dip varies with the distance. The size of such a device can be reduced to the scale of a few millimeters to enable fabrication of an on-chip spectrometer for micro total analysis systems (μ-TAS). A light beam impinging on a CPhC film is reflected only at wavelengths that coincide with the stop band at a specific position. By measuring the transmission intensity profile over the whole area of the CPhC film using a CMOS sensor array, the spectrum of the incident light can be analyzed. We employed a composite film instead of a porous film because the composite film yielded a higher transparency and a FWHM of the reflectance spectrum smaller than 11 nm, which enhanced the resolution of the spectrometer. Optical microscopy images of the composite CPhC films with gradients in blue-green and red colors and the evolution of their stop bands as a function of distance along the gradient is shown in Figure 4a,b (see Figure S2 in the Supporting Information for details). The blue-green and red films were prepared by diffusion of 153 and 205 nm silica particles, and the slopes of the wavelength evolution as a function of distance were 29.3 $nm\,mm^{-1}$ and 17.5 $nm\,mm^{-1}$, respectively. The background greyscale images shown in Figure 4 are CPhC film-mounted CMOS images collected under illumination with light of a narrow bandwidth of approximately 0.1 nm. The gradient of the blue-green film was illuminated by a beam centered at 490–534 nm in wavelength intervals of 1 nm, whereas the red film was illuminated with a beam centered at 645–710 nm. The dark regions in each CMOS image were matched with the stop band position, the wavelength at the transmission dip. The movie S1 in the Supporting Information shows that the dark region in the CMOS images shifts in the composite CPhC red film. A beam centered at 670–680 nm in wavelength intervals of 0.25 nm yielded a one-to-one correspondence between the distance and the wavelength, as shown in Figure S3 in the Supporting Information. This result provides evidence of a resolution limit smaller than 0.25 nm. Because the CMOS camera pixels were $5.2\,\mu m\times5.2\,\mu m$ in area, the ultimate resolution limit of the device was estimated to be 0.09 nm.

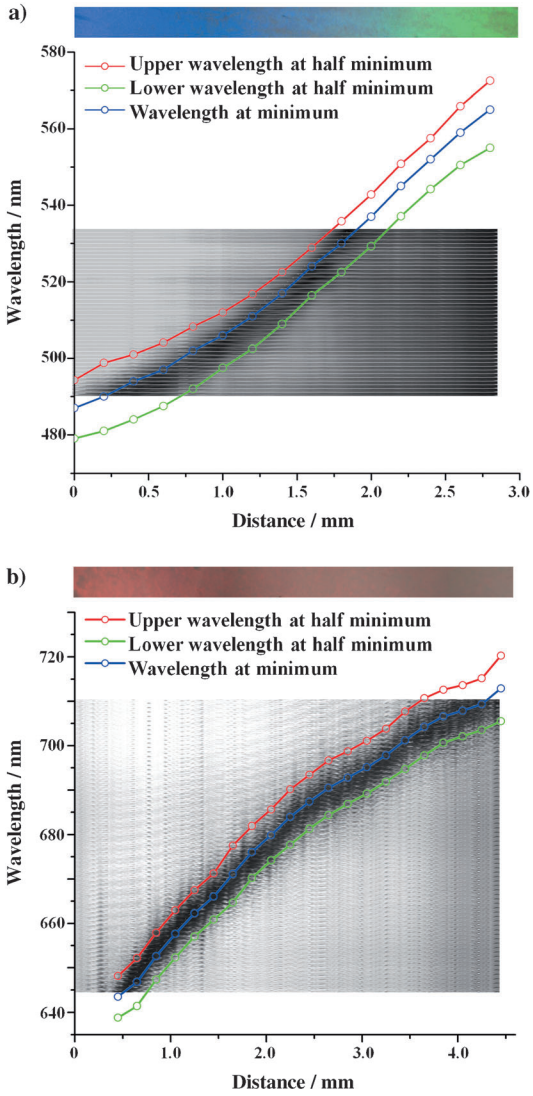

Figure 4. a) A set of optical microscopy images and the evolution of the dip wavelength and upper and lower wavelengths at the half-minimum in the transmittance spectra of a composite blue-green gradient film as a function of the distance. The image in the graph shows a collection of 45 CMOS images gathered under illumination with light of a narrow bandwidth of 0.1 nm centered at 490–534 nm. The evolution of the dip wavelength is in good accord with the darkest position of the CMOS images. b) Same set of images for the composite red CPhC film, where the image in the graph is composed of 66 CMOS images obtained by illuminating with light centered at 645–710 nm.

The CPhC materials may potentially be used in a variety of tunable photonic devices as well as spectrometers although the CPhC film can have imperfections in crystal structures. For example, tunable optical filters or reflectors can be prepared using CPhC films equipped with microcontrollers. In addition, CPhC films can be used in photonic crystal laser cavities to permit the continuous modulation of the lasing wavelength.[14] This diffusion-based novel approach to fabricating CPhCs shows promise for a wide range of photonic applications owing to its unique properties, high degree of controllability, and simplicity of preparation. We expect that diffusion-driven structural transformations may open new avenues for engineering the optical properties of 3D photonic crystals.

Experimental Section

Preparation of the photocurable suspension: Monodisperse silica particles 153, 177, and 205 nm in diameter were synthesized by sol–gel chemistry according to the Stöber–Fink–Bohn method. The silica suspension was washed twice with ethanol and then mixed with ETPTA (SR454, Sartomer) containing 0.2 wt% 2-hydroxy-2-methyl-1-phenyl-1-propanone (HMPP; Darocur1173, Ciba Chemical) as a photoinitiator. The ethanol was selectively evaporated at 70°C in a convection oven for 1 day, followed by cooling to room temperature with sonication for 30 min.

Formation of a color gradient: A glass cell 5 cm in length, 7 mm in width, and 50 μm in height was prepared from two glass slides separated by a spacer of 50 μm thick polyimide tape (Kapton). Into the channel, particle-free ETPTA was introduced by capillary action, and residual ETPTA at the entrance was removed. A silica–ETPTA suspension was subsequently introduced at the same entrance. After specific diffusion times, the channel was exposed to ultraviolet light for 10 seconds to polymerize the ETPTA. The silica particles embedded in ETPTA were selectively etched away by immersing the composite film in 5% HF solution (Sigma–Aldrich) for 12 h.

Characterization: The photonic crystal films displaying color gradients were observed by optical microscopy (Nikon, L150) and SEM (Philips, XL30). The reflection spectra were measured using an optical spectrometer (Ocean Optics, USB4000) mounted to an optical microscope while transmission spectra were collected using an optical setup consisting of a monochromator (Spectral Products, DK240) and a Si photodetector (New Focus, Visible Femtowatt Photoreceiver). To demonstrate the miniaturized spectrometer, we mounted a composite CPhC film on a CMOS camera (Thorlabs, DCC1545M). The space between the film and the sensor array was filled with pure ETPTA to minimize undesired reflection and refraction at the interfaces. The light sources of the narrow bandwidth (0.1 nm) were generated using a combination of a tungsten lamp source and a monochromator (Spectral Products, DK240) with a focal length of 240 mm, groove density of 1200 $g\,mm^{-1}$, and with entrance and exit slits 100 μm in width.

Received: June 29, 2011
Published online: September 14, 2011

Keywords: colloidal crystals · diffusion · photonic crystals

[1] a) Y. Monovoukas, A. P. Gast, *J. Colloid Interface Sci.* **1989**, *128*, 533; b) S. A. Asher, J. Holtz, L. Liu, Z. Wu, *J. Am. Chem. Soc.* **1994**, *116*, 4997; c) M. E. Leunissen, C. G. Christova, A.-P. Hynninen, C. P. Royall, A. I. Campbell, *Nature* **2005**, *437*, 235.
[2] J. Holtz, S. A. Asher, *Nature* **1997**, *389*, 829.
[3] J. R. Lawrence, Y. Ying, P. Jiang, S. H. Foulger, *Adv. Mater.* **2006**, *18*, 300.
[4] S.-H. Kim, S.-G. Jeon, W. C. Jeong, H. S. Park, S.-M. Yang, *Adv. Mater.* **2008**, *20*, 4129.
[5] a) P. Jiang, J. F. Bertone, K. S. Hwang, V. L. Colvin, *Chem. Mater.* **1999**, *11*, 2132; b) Y. A. Vlasov, X.-Z. Bo, J. C. Sturm, D. J. Norris, *Nature* **2001**, *414*, 289.
[6] S. A. Rinne, F. Garcia-Santamaria, P. V. Braun, *Nat. Photonics* **2008**, *2*, 52.
[7] a) S.-K. Lee, G.-R. Yi, J. H. Moon, D. J. Pine, S.-M. Yang, *Adv. Mater.* **2006**, *18*, 2111; b) H. Kim, J. Ge, J. Kim, S.-E. Choi, H. Lee, H. Lee, W. Park, Y. Yin, S. Kwon, *Nat. Photonics* **2009**, *3*, 534.

[8] a) F. Marlow, Muldarisnur, P. Sharifi, R. Brinkmann, C. Mendive, *Angew. Chem.* **2009**, *121*, 6328; *Angew. Chem. Int. Ed.* **2009**, *48*, 6212; b) S.-H. Kim, S. Y. Lee, S.-M Yang, G.-R. Yi, *NPG Asia Mater.* **2011**, *3*, 25.
[9] a) B. Gates, Y. Xia, *Adv. Mater.* **2000**, *12*, 1329; b) T. Kanai, T. Sawada, J. Yamanaka, K. Kitamura, *J. Am. Chem. Soc.* **2004**, *126*, 13210.
[10] W. B. Russel, D. A. Saville, W. R. Schowalter, *Colloidal dispersion* Cambridge, University Press, New York, **1999**, chap. 13.
[11] a) S. R. Raghavan, H. J. Walls, S. A. Khan, *Langmuir* **2000**, *16*, 7920; b) J. Ge, Y. Yin, *Adv. Mater.* **2008**, *20*, 3485.
[12] J. R. Lawrence, G. H. Shim, P. Jiang, M. G. Han, Y. Ying, S. H. Foulger, *Adv. Mater.* **2005**, *17*, 2344.
[13] a) S.-H. Kim, H. S. Park, J. H. Choi, J. W. Shim, S.-M. Yang, *Adv. Mater.* **2010**, *22*, 946; b) N. K. Pervez, W. Cheng, Z. Jia, M. P. Cox, H. M. Edrees, I. Kymissis, *Opt. Express* **2010**, *18*, 8277.
[14] a) M. N. Shkunov, Z. V. Vardeny, M. C. DeLong, R. C. Polson, A. A. Zakhidov, R. H. Baughman, *Adv. Funct. Mater.* **2002**, *12*, 21; b) S.-H. Kim, S.-H. Kim, W. C. Jeong, S.-M. Yang, *Chem. Mater.* **2009**, *21*, 4993.

